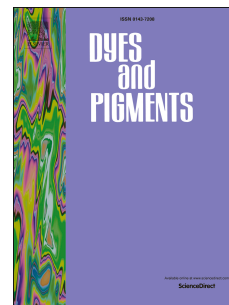


Journal Pre-proof

Ratiometric fluorescent sensor based oxazolo-phenazine derivatives for detect hypochlorite via oxidation reaction and its application in environmental samples

You-Ming Zhang, Hu Fang, Wei Zhu, Jun-Xia He, Hong Yao, Tai-Bao Wei, Qi Lin, Wen-Juan Qu



PII: S0143-7208(19)31360-9

DOI: <https://doi.org/10.1016/j.dyepig.2019.107765>

Reference: DYPI 107765

To appear in: *Dyes and Pigments*

Received Date: 12 June 2019

Revised Date: 31 July 2019

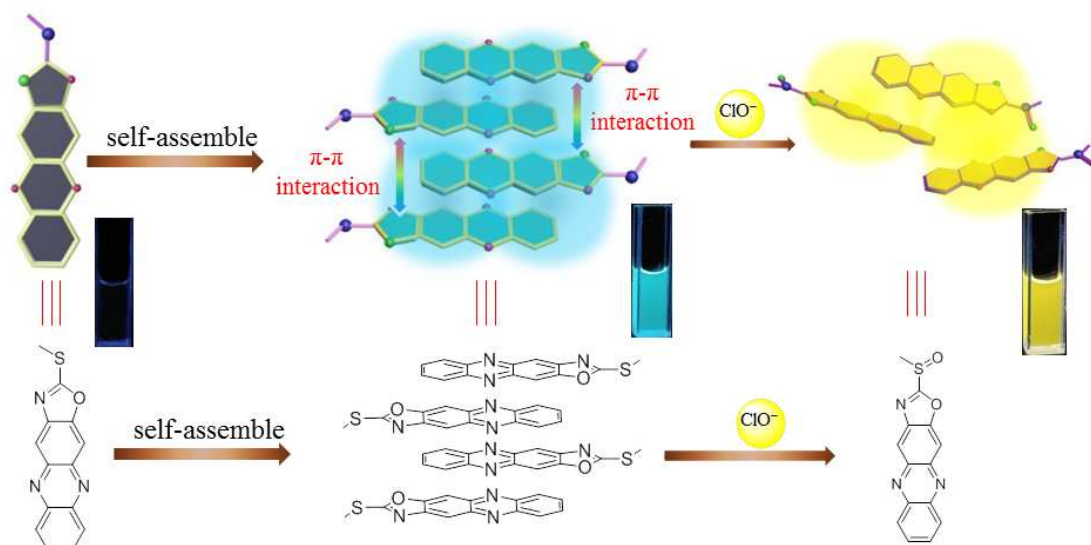
Accepted Date: 31 July 2019

Please cite this article as: Zhang Y-M, Fang H, Zhu W, He J-X, Yao H, Wei T-B, Lin Q, Qu W-J, Ratiometric fluorescent sensor based oxazolo-phenazine derivatives for detect hypochlorite via oxidation reaction and its application in environmental samples, *Dyes and Pigments* (2019), doi: <https://doi.org/10.1016/j.dyepig.2019.107765>.

This is a PDF file of an article that has undergone enhancements after acceptance, such as the addition of a cover page and metadata, and formatting for readability, but it is not yet the definitive version of record. This version will undergo additional copyediting, typesetting and review before it is published in its final form, but we are providing this version to give early visibility of the article. Please note that, during the production process, errors may be discovered which could affect the content, and all legal disclaimers that apply to the journal pertain.

© 2019 Published by Elsevier Ltd.

Graphical abstract



In this work, we designed and synthesized a phenazine derivative (**POC**) based fluorescent sensor which could high selectivity detect hypochlorite in DMSO/ H_2O (3:7, v/v) solution.

Ratiometric fluorescent sensor based oxazolo-phenazine derivatives for detect hypochlorite via oxidation reaction and its application in environmental samples

You-Ming Zhang^{a,b*}, Hu Fang^a, Wei Zhu^a, Jun-Xia He^a, Hong Yao^a, Tai-Bao Wei^a,
Qi Lin^a, Wen-Juan Qu^{a*}

^a Key Laboratory of Eco-Environment-Related Polymer Materials, Ministry of Education of China;
Key Laboratory of Polymer Materials of Gansu Province; College of Chemistry and Chemical
Engineering, Northwest Normal University, Lanzhou, Gansu, 730070. P. R. China

^b College of chemistry and Chemical Engineering, Lanzhou City University, Lanzhou, Gansu,
730070, P. R. China

Abstract

In this work, we designed and synthesized a ratiometric fluorescent sensor (**POC**) based phenazine derivative which can specifically detect hypochlorite (detection limit equals to 8.9×10^{-7} M) in DMSO/H₂O (3:7, v/v) solution. With addition of hypochlorite to the solution of **POC**, hypochlorite broken π - π stacking of **POC**, and then oxidizes sulfur atoms in phenazine groups to sulfoxide, which resulted in the fluorescent color changed from blue to yellow. Job's plot showed that binding stoichiometry of **POC** with ClO⁻ was 2:1. In addition, **POC** could be used to real-time detect hypochlorite in environment samples, and the naked eyes detection limit reached up to 7×10^{-5} M.

*Corresponding author

Tel: +086 9317973191; E-mail address: zhangnwnu@126.com (You-Ming Zhang)

*Corresponding author

E-mail address: quwenjuanlz@163.com (Wen-Juan Qu)

Keywords: Phenazine derivative; hypochlorite; ratiometric fluorescent sensor; oxidation reaction; environmental samples

1. Introduction

It is well known that hypochlorite has strong oxidizing properties under acidic or alkaline conditions and it could be used as bactericidal agent [1]. Nowadays, hypochlorite has been widely used in household bleaching, disinfection of drinking water and swimming pools. It is worth mentioning that using appropriate amount of hypochlorite could provide us a clean environment, safe drinking water and served as an effective antibacterial agent in life [2, 3]. However, hypochlorite is also a double-edged sword. Residual hypochlorite in water could enter the living body through some routes and then enriched [4], which may induce oxidative stress and oxidative damage, even cause more serious diseases such as arthritis and cardiovascular disease, hard atheroma, neuronal degeneration and cancer [5-11]. Hence, it is urgent needed to develop a novel method for efficiently detecting hypochlorite in environmental samples.

Methods for detection of hypochlorite included normalized iodometric titration [12], electrochemical analysis [13], spectrophotometry [14], chemiluminescence [15], and colorimetric chemosensor [16]. However, these detection methods require expensive instruments and were not easy to promote. In recent years, fluorescent sensors have become popular [17-20]. Fluorescent sensors based on small organic molecules have attracted wide attention of researchers because of their low cost, simple synthesis and easy operation [21-27]. Up to now, a large number of organic fluorescent sensors have

been developed, but ratiometric fluorescence sensors which could be used to sensitive and convenient detect hypochlorite have been rarely reported [28-34].

Phenazine and its derivatives were used as raw materials for organic synthesis and dye intermediates widely used in daily life and work [35-40]. At the same time, phenazine derivatives could be used as ionic ligands and hydrogen bond acceptors because of their own structural characteristics (containing electron-deficient π system, with the pair of electron-bearing nitrogen atoms and three fused aromatic rings). It was also beneficial for π - π electrons to overlap each other, so a kind of compound has considerable application prospects in supramolecular chemistry [41-46]. Therefore, combining with our previous works [47, 48], we designed and synthesized 2-(methylthio)oxazolo[4,5-b]phenazine (**POC**) as novel ratiometric fluorescent sensor (Scheme1), which could high sensitivity and selectivity identification hypochlorite through oxidation reaction. Adding hypochlorite to **POC** in the DMSO/H₂O (3:7, v/v) solution, hypochlorite broken π - π stacking of **POC**, and then oxidizes sulfur atoms in phenazine groups to sulfoxide, fluorescence color of **POC** solution changed from green to yellow.

As we all know, the active ingredient of 84 disinfectant was hypochlorite. We diluted the 84 disinfectant (jing bai li[®]) with tap water, and then added different concentrations of 84 disinfectant to **POC** (20 μ M) solution to observe the color change. The naked-eyes detection limit of **POC** to 84 disinfectant was 7×10^{-5} M under the UV lamp (365 nm). So **POC** could be applied to the on-site and real-time monitoring of hypochlorite in daily-life samples.

Scheme1**2. Experimental section***2.1. Materials*

All reagents were analytical grade, commercially and without further purification. UV-vis spectra were recorded on a Shimadzu UV-2550. Fluorescence spectra were recorded on a Shimadzu RF-5301PC. ^1H NMR spectra were recorded on a Mercury-400BB spectrometer at 400 MHz with $\text{DMSO-}d_6$ as solvent. Chemical shifts are reported in ppm downfield from tetramethylsilane (TMS, δ scale with solvent resonances as internal standards). Mass spectra were performed on a Bruker Esquire 3000 plus mass spectrometer (Bruker-FranzenAnalytik GmbH Bremen, Germany) equipped with ESI interface and ion trap analyzer.

*2.2. Synthesis and characterization of sensor **POC***

A mixture of oxazolo[4,5-b]phenazine-2-thiol (0.253 g, 1 mmol), K_2CO_3 (0.138 g, 1 mmol), KI (1.992 g, 1.2 mmol), methyl iodide (0.171 g, 1.2 mmol) and acetonitrile (50 mL) were added to a 100 mL round-bottom flask under nitrogen atmosphere. The reaction mixture was stirred at 80°C for 72h. The crude product was purified by silica gel column chromatography using petroleum ether/ethyl acetate (v/v = 50:1) as the eluent, compound **POC** as yellow solid (0.234 g, yield 88%) was isolated, m.p. $263\text{--}265^\circ\text{C}$ ^1H NMR (Figure S1) (400 MHz, $\text{DMSO-}d_6$) δ 8.35 (s, 2H, ArH), 8.25 (s, 2H, ArH), 7.96 (d, $J = 3.2$ Hz, 2H, ArH), 2.89 (d, $J = 2.5$ Hz, 3H, SCH_3). ^{13}C NMR (151 MHz, CDCl_3), δ/ppm : 172.66, 142.83, 142.74, 141.72, 141.35, 130.18, 130.12,

129.38, 129.19, 115.15, 105.96, 14.70. ESI-MS m/z : Calcd for $C_{14}H_{10}N_3OS$ [$POC + H$] $^+$: 268.0545; Found 268.0542 (Figure S2).

2.3. Preparation of solutions of ROS and anions

The ROS (reactive oxygen species) including $NO\bullet$, $\bullet O^{2-}$, $ONOO^-$, H_2O_2 , $OH\bullet$, $t\text{-BuOOH}$ and ClO^- were prepared as follows: $NaClO$ was prepared by diluting with 8% aqueous solution, and final concentration is 1.0×10^{-2} M. H_2O_2 was obtained by diluting with 30% aqueous solution, and final concentration is 1.0×10^{-2} M. Nitric oxide radical ($NO\bullet$) was generated from SNP (sodium nitrofer-ricyanide (III) dihydrate). SNP was added to deionized water and then stirred for 1 h at room temperature. Hydroxyl radical ($OH\bullet$) was generated by the Fenton reaction. To prepare $OH\bullet$ solution, $FeSO_4$ was added in the presence of 50 μM of H_2O_2 . With deionized water, a 70% solution was diluted to prepare tert-butyl hydroperoxide ($t\text{-BuOOH}$). The superoxide radical ($\bullet O^{2-}$) was generated from improved 1,2,3-trihydroxybenzene autoxidation method, the pyrogallol solution (in 1 M HCl) was thoroughly mixed with pH 7.4 Tris-HCl buffer. Peroxynitrite ($ONOO^-$) was prepared by the reaction of hydrogen peroxide with sodium nitrite. Sodium salt (1.0×10^{-2} M) of anions (F^- , Cl^- , I^- , SCN^- , ClO_3^- , BrO_3^- , and IO_3^-) and potassium salt (1.0×10^{-2} M) of anions (Br^- , $H_2PO_4^-$, HPO_4^{2-} , PO_4^{3-} , $P_2O_7^{4-}$, $P_3O_{10}^{5-}$, HSO_4^- , SO_3^{2-} , SO_4^{2-} , $S_2O_3^{2-}$, S^{2-} , N^{3-} , NO_3^- , NO_2^- , $C_2O_4^{2-}$, CO_3^{2-} , AcO^- , and $B_4O_7^{2-}$) was prepared in twice-distilled water.

Figure 1; Figure 2

3. Results and Discussion

3.1. Self-assembly study

At the beginning, we investigated the self-assembly procedure of **POC** in DMSO-H₂O binary solution. As shown in Figure 1, the **POC** (20 μ M) could dissolve in DMSO solution and no fluorescence. With water content increases, the emission intensity at 489 nm increased gradually and the green fluorescence appeared. The emission intensity was maximized when the water content reaches 70%. Regrettably, as the water content continues to increase, the fluorescence intensity at 489 nm decreases gradually. According to the related reports [49-51], we speculate that **POC** has π - π stacking interactions in DMSO-H₂O binary system (Scheme 2). Meanwhile, the XRD spectra supported this proposed mechanism in Figure S4. The free sensor **POC** has a peak at $2\theta=23.7^\circ$, corresponding to d-spacing of 3.81 Å, which indicated that π - π stacking interactions existed in **POC**. Based on the above tests, we determined that the **POC** could self-assemble via π - π stacking interactions in DMSO-H₂O binary system.

3.2. Photophysical properties of sensor **POC**

We carried out its UV-vis absorption experiments. As shown in Figure S5, sensor **POC** (20 μ M) with and without ClO⁻ were observed in DMSO/H₂O (3:7, v/v) solution, the free sensor **POC** have a strong absorption peak at 390 nm. Interestingly, when excess ClO⁻ were added to the sensor **POC** (20 μ M) solution, the absorption peak at 390 nm decreased and a broad shoulder peak appeared at 430 nm. Meanwhile, the color of **POC** solution changed from colorless to pale yellow. In addition,

fluorescence spectra of sensor **POC** with and without ClO^- were observed in DMSO/ H_2O (3:7, v/v) solution. As shows in Figure 2, sensor **POC** (20 μM) exhibits a strong emission peak at 489 nm, delightfully, fluorescence emission from a solution of **POC** undergoes a 61 nm red-shift upon addition of ClO^- , and fluorescence color dramatically changed from green to yellow. Subsequently, we investigated the ability of the sensor molecule **POC** for detect hypochlorite in different DMSO- H_2O binary solution. As shown in Figure S6 the sensor of **POC** showed good detection ability for hypochlorite under different DMSO- H_2O binary solution, with the increase of water content, the emission intensity at 520 nm gradually decreases. And time-dependent variations in the fluorescence emission spectroscopes were monitored in the presence of 50 equivalents of ClO^- , as shown in Figure S7. The kinetic study showed that the reaction was completed within 18 min for ClO^- . What's more, with the time extension, the intensity ratio (F_{489}/F_{550}) remains unchanged.

Figure 3

3.3. Sensitivity studies

The interaction between **POC** and ClO^- was further investigated through fluorescence titration methods by adding a standard solution of corresponding ions to a DMSO/ H_2O (3:7, v/v) solution of the **POC** (2.0×10^{-5} M). As shown in Figure 3, Upon addition of ClO^- (0-122 equiv.), an isosbestic point at 520 nm was clearly observed with increasing concentrations of hypochlorite, at the same time, the emission intensity at 489 nm gradually decreased as well as the emission intensity at

550 nm increased gradually. The ratio of the fluorescence intensities at 489 and 550 nm (F_{489}/F_{550}) decreases 33-fold upon addition of 122 equivalents ClO^- . Moreover, in order to further determine the detection limit of the **POC** to ClO^- , the fluorescence spectrum of the blank test was measured 20 times, and the standard deviation of the blank measurement was calculated. The linear fitting was performed according to the fluorescence titration curve to determine the slope (Figure S8). The detection limit was calculated using the following equation: Detection limit = $3\sigma/S$. The detection limit of **POC** to hypochlorite was 8.9×10^{-7} M. We have compared the **POC** with other reported sensors. We found that the response time of **POC** for ClO^- was 18 min, which was longer than other reported sensors, but the sensitivity of **POC** for ClO^- was higher than other reported sensors.

Figure 4

3.4. Selectivity studies

In order to investigate the selectivity of **POC** to ClO^- , we measured the fluorescence intensive of **POC** in the presence of various analytical substrates (F^- , Cl^- , I^- , SCN^- , ClO_3^- , BrO_3^- , IO_3^- , Br^- , H_2PO_4^- , HPO_4^{2-} , PO_4^{3-} , $\text{P}_2\text{O}_7^{4-}$, $\text{P}_3\text{O}_{10}^{5-}$, HSO_4^- , SO_3^{2-} , SO_4^{2-} , $\text{S}_2\text{O}_3^{2-}$, S^{2-} , N^{3-} , NO_3^- , NO_2^- , $\text{C}_2\text{O}_4^{2-}$, CO_3^{2-} , AcO^- , $\text{B}_4\text{O}_7^{2-}$, ClO^- , and H_2O_2). As shown in Figure 4, after addition of hypochlorite to **POC**, the maximum fluorescence emission peak of **POC** was red-shifted from 489 nm to 550 nm, while other analytical substrates showed no change in maximum fluorescence emission peak. Competition experiments also showed that other analytes had no effect on **POC**

detection hypochlorite. As shown in Figure 5, the ratio of intensity ratio (F_{489}/F_{550}) was hardly changed by adding 50 equivalents of other analytical substrates to the solution of **POC**- ClO^- . Subsequently, we measured the fluorescence intensive of **POC** in the presence of various reactive oxygen species (including $\text{NO}\cdot$, $\cdot\text{O}^{2-}$, ONOO^- , H_2O_2 , $\text{OH}\cdot$, t-BuOOH and ClO^-). As shown in Figure S9 and Figure S10, Only ClO^- responds to **POC**, competition experiments also showed that other reactive oxygen species had no effect on **POC** detection hypochlorite. The above experiments showed that **POC** could high selectivity detect hypochlorite.

Figure 5

3.5. The effect of pH

To further confirm the practical applicability of **POC**, pH effect on the performance of **POC** toward ClO^- was investigated from pH 2 to 13 in DMSO/ H_2O (3:7, v/v) HEPES buffered solution. The results were depicted in Figure S11, Figure S12 and S13. In the absence of ClO^- , the intensity ratio of the sensor **POC** (F_{489}/F_{550}) drastically reduced at $\text{pH} > 11$, but in the presence of ClO^- , the intensity ratio of the sensor **POC** (F_{489}/F_{550}) remained unchanged in a broad pH range. These results indicated that ClO^- could be clearly detected by fluorescence spectral measurement using **POC** in the broad pH range of 2-10.

3.6. Stoichiometric relationship studies

In order to determine the stoichiometric relationship between **POC** and ClO^- , job plot was obtained. The method was that keeping total concentration of **POC** and ClO^-

at 10.0 μM in DMSO/H₂O (3:7, v/v) solution, and changing the molar ratio of ClO⁻ (X_M ; $X_M = [\text{ClO}^-]/\{[\text{POC}] + [\text{ClO}^-]\}$) from 0 to 1. As shown in Figure 6, the fluorescence intensity at 550 nm was plotted against molar fraction of **POC** sensor. The maximum emission intensity was reached when the molar fraction was 0.3. This result illuminated that binding stoichiometry of **POC** with ClO⁻ was 2:1. The same result was obtained for the ¹H NMR titration experiment. As shown in Figure 7, when 0.5 equivalents ClO⁻ were added to **POC**, the signal peak at 2.89 ppm was shifted to 2.93 ppm.

Scheme 2

3.7. Sensing mechanism

It is well known that under certain oxidizing agents, thioether groups can be oxidized to sulfoxide groups, sulfones groups, and even sulfonates. According to previous reports [52, 53], we proposed a reasonable mechanism for the detection of hypochlorite by **POC** in aqueous solution. As shown in scheme 2, with addition of hypochlorite to the solution of **POC**, hypochlorite broken π - π stacking of **POC**, and then oxidizes sulfur atoms in phenazine groups to sulfoxide. In order to further verify the proposed response mechanism, we performed XRD, ¹H NMR and mass spectrometry measurements. The above self-assembly mechanism was confirmed by XRD (Figure S4). The free sensor **POC** have a peak at $2\theta=23.7^\circ$, corresponding to a d-spacing of 3.81Å, indicating that π - π stacking interactions exists in **POC**. In addition, compared to **POC**-ClO⁻, this peak was significantly decreased. The

experiments showed that hypochlorite leads to π - π stacking decreased. The ^1H NMR titration experiment was recorded, as shown in Figure 7, with the addition of hypochlorite to **POC** solution, H^{d} (2.89 ppm) signal peak in $\text{DMSO-}d_6$ gradually disappeared, and when 0.5 equivalent of ClO^- was added, a new signal peak appeared at 2.93 ppm, the signals of H^{a} (8.34 ppm), H^{b} (8.24 ppm) and H^{c} (7.96 ppm) showed downfield shifts (shifted to 8.38 ppm, 8.29 ppm, 8.02 ppm, respectively), which indicated that with the addition of hypochlorite, the electronegativity of **POC** increases, and peak of **POC** signal shift to downfield field. To further verify rationality of sensing mechanism, we tested the reaction mixture of **POC** and ClO^- by mass spectrometer. To our delight, Figure S14 manifests an increased molecular weight of 16, which is equal to the molecular weight of oxygen. The above experiments supported our proposed sensing mechanism. Hypochlorite broken π - π stacking of **POC**, and then oxidizes sulfur atoms in phenazine groups to sulfoxide.

Figure 6

3.8. **POC** detection of 84 disinfectant

Based on above experiment results, we further investigated the applicability of sensor **POC** for detecting hypochlorite in daily life relevant samples. We prepared a commercially available 84 disinfectant (jing bai li[®]) as analytical substrate. As shown in Figure S15, we added different concentrations of hypochlorite disinfectant solution to 20 μM **POC** $\text{DMSO}/\text{H}_2\text{O}$ (3:7, v/v) solution. When concentrations reached 7×10^{-6} M, the fluorescent color of solution couldn't change obviously. Thus the naked-eyes

detection limit of **POC** to hypochlorite was 7×10^{-5} M under the UV lamp (365 nm). In order to investigate the practical application of sensor **POC**, test strips were prepared by immersing filter papers into DMSO/H₂O (3:7, v/v) solution of **POC** (2×10^{-4} M) and then drying in air. As shown in Figure S16, when 84 disinfectant and other ions were added to the test kit, the obvious color changes was observed only with 84 disinfectant under the UV-lamp (365 nm), and potentially competitive analytical substrates did not affect the detection of the disinfectant solution by the test strip. Therefore, **POC** provides a possibility for detecting hypochlorite disinfectants on-site in daily life, and **POC** test strip could be used as an effective tool for detecting hypochlorite in real time.

Figure 7

4. Conclusion

In summary, a novel ratiometric fluorescent sensor for highly selective and sensitive detection hypochlorite based on phenazine derivative was designed and synthesized, which could be used as a fluorescent response sensor for hypochlorite in DMSO/H₂O (3:7, v/v) solution. Detailed mechanism studies indicate that addition of hypochlorite, hypochlorite broken π - π stacking of **POC**, and then oxidizes sulfur atoms in phenazine groups to sulfoxide. The detection limit of **POC** to hypochlorite was as low as 8.9×10^{-7} M in aqueous solution. In addition, **POC** could detect 84 disinfectant in aqueous solution, and naked-eyes detection limit was 7×10^{-5} M. **POC** test strips could be applied to detect hypochlorite rapidly of hypochlorite in the

disinfectant. In view of this, we designed and synthesized a phenazine derivative-based ratiometric fluorescent sensor molecule **POC**, which provides a practical method for the detection of hypochlorite in daily life samples.

Acknowledgements

This work was supported by the National Natural Science Foundation of China (NSFC) (Nos. 21574104; 21662031; 21661028), the Natural Science Foundation of Gansu Province (1506RJZA273) and the Program for Changjiang Scholars and Innovative Research Team in University of Ministry of Education of China (IRT15R56).

References

- [1] Halliwell B, Aeschbach R, Löliger J, Aruoma OI. The characterization of antioxidants. *Food Chem Toxicol* 1995;33:601-17.
- [2] Mosci D, Marmo GW, Sciolino L, Zaccaro C, Antonellini R, Accogli L, Lazzarotto T, Mongardi M, Landini MP. Automatic environmental disinfection with hydrogen peroxide and silver ions versus manual environmental disinfection with sodium hypochlorite: a multicentre randomized before-and-after trial. *J Hosp Infect* 2017;97:175-9.
- [3] Wang BH, Chen D, Kambam S, Wang F, Wang Y, Zhang W, Yin J, Chen HY, Chen XQ. A highly specific fluorescent probe for hypochlorite based on fluorescein derivative and its endogenous imaging in living cells. *Dyes Pigments* 2015;120:22-9.

- [4] Prokopowicz ZM, Arce F, Biedron R, Chiang CL, Ciszek M, Katz DR, Nowakowska M, Zapotoczny S, Marcinkiewicz J, Chain BM. Hypochlorous acid: a natural adjuvant that facilitates antigen processing, crosspriming, and the induction of adaptive immunity. *J Immunol* 2010;184:824-835.
- [5] Yap YW, Whiteman M, Cheung NS. Chlorinative stress: an under appreciated mediator of neurodegeneration. *Cell Signal* 2007;19:219-28.
- [6] Pattison DI, Davies MJ. Evidence for rapid inter and intramolecular chlorine transfer reactions of histamine and carnosine chloramines: implications for the prevention of hypochlorous-acid-mediated damage. *Biochemistry* 2006;45:8152-62.
- [7] Hazen SL, Heinecke JW. 3-chlorotyrosine, a specific marker of myeloperoxidase-catalysed oxidation, is markedly elevated in low-density lipoprotein isolated from human atherosclerotic intima. *J Clin Invest* 1997;99:2075-81.
- [8] Zheng L, Nukuna B, Brennan ML, Sun M, Goormastic M, Settle M, Schmitt D, Fu X, Thomson L, Fox PL, Ischiropoulos H, Smith JD, Kinter M, Hazen SL. J. Apolipoprotein A-I is a selective target for myeloperoxidase-catalyzed oxidation and functional impairment in subjects with cardiovascular disease. *Clin Invest* 2004;114:529-41.
- [9] Weitzman SA, Gordon LI. Inflammation and cancer: role of phagocyte-generated oxidants in carcinogenesis. *Blood* 1990;76:655-63.

- [10] Hasegawa T, Malle E, Farhood A, Jaeschke H. Generation of hypochlorite-modified proteins by neutrophils during ischemia-reperfusion injury in rat liver: attenuation by ischemic preconditioning. *Am J Physiol Gastrointest Liver Physiol* 2005;289:760-7.
- [11] Malle E, Buch T, Grone HJ. Myeloperoxidase in kidney disease. *Kidney Int* 2003;64:1956-67.
- [12] Wright PP, Kahler B, Walsh LJ. The Effect of Heating to Intracanal Temperature on the Stability of Sodium Hypochlorite Admixed with Etidronate or EDTA for Continuous Chelation. *J Endodont* 2019;45:57-61.
- [13] Thiagarajan S, Wu ZY, Chen SM. Amperometric determination of sodium hypochlorite at poly MnTAPP-nano Au film modified electrode. *J Electroanal Chem* 2011;661:322-8.
- [14] Soto NO, Horstkotte B, March JG, Pl LDA, López ML, Cerdá MV. An environmental friendly method for the automatic determination of hypochlorite in commercial products using multisyringe flow injection analysis. *Anal Chim Acta* 2008;611:182-6.
- [15] Claver JB, Mirón MCV, Capitán-Vallvey LF. Determination of hypochlorite in water using a chemiluminescent test strip. *Anal Chim Acta* 2004;522:267-73.
- [16] Lou X, Zhang Y, Qin J, Li Z. Colorimetric hypochlorite detection using an azobenzene acid in pure aqueous solutions and real application in tap water. *Sens Actuators B* 161;2012:229-34.

- [17] Huang K, Jiao X, Liu C, Wang Q, Qiu X, D. Zheng, He S, Zhao L, Zeng X. Highly selective and sensitive fluorescent probe for mercury ions based on a novel rhodol-coumarin hybrid dye. *Dyes Pigments* 2017;142:437-46.
- [18] Li W, Wang L, Tang H, Cao D. Diketopyrrolopyrrole-based fluorescent probes for detection and bioimaging: Current progresses and perspectives. *Dyes Pigments* 2019;162:934-50.
- [19] Wu L, Yang Q, Liu L, Sedgwick AC, Cresswell AJ, Bull SD, Huang C, James TD. ESIPT-based fluorescence probe for the rapid detection of hypochlorite (HOCl/ ClO), *Chem. Commun. Chem Commun* 2018;54:8522-5.
- [20] Li T, Wang L, Lin S, Xu X, Liu M, Shen S, Yan Z, Mo R. Rational Design and Bioimaging Applications of Highly Specific “Turn-On” Fluorescent Probe for Hypochlorite. *Bioconjugate Chem* 2018;29:2838-45.
- [21] Pak YL, Park SJ, Xu Q, Kim HM, Yoon J. Ratiometric Two-Photon Fluorescent Probe for Detecting and Imaging Hypochlorite. *Anal Chem* 2018;90:9510-4.
- [22] Fu ZH, Han X, Shao Y, Fang J, Zhang ZH, Wang YW, Peng Y. Fluorescein-based Chromogenic and Ratiometric Fluorescence Probe for Highly Selective Detection of Cysteine and Its Application in Bioimaging. *Anal Chem* 2017;89:1937-44.
- [23] Li JW, Yin CX, Huo FJ, Xiong KM, Chao JB, Zhang YB. Two high selective and sensitive ratiometric fluorescence probes for detecting hypochlorite. *Sens Actuators B* 2016;231:547-51.

- [24] Cui W, Wang L, Xiang G, Zhou L, An X, Cao D. A colorimetric and fluorescence “turn-off” chemosensor for silver ion detection based on a conjugated polymer containing 2,3-di(pyridin-2-yl)quinoxaline. *Sens Actuators B* 2015;207:281-90.
- [25] Fu ZH, Yan LB, Zhang X, Zhu FF, Han XL, Fang J, Wang YW, Peng Y. A Fluorescein-Based Chemosensor for Relay Fluorescence Recognition of Cu(II) Ions and Biothiols in Water and Its Applications to Molecular Logic Gate and Living Cell Imaging. *Org Biomol Chem* 2017;15:4115-21.
- [26] Kang JH, Han J, Lee H, Lim MH, Kim KT, Kim C. A water-soluble fluorescence chemosensor for the sequential detection of Zn^{2+} and pyrophosphate in living cells and zebrafish. *Dyes Pigments* 2018;152:131-8.
- [27] Hwang SM, Kim A, Kim C. A simple hydrazine-based probe bearing anthracene moiety for the highly selective detection of hypochlorite. *Inorg Chem Commun* 2019;101:1-5.
- [28] Pak YL, Park SJ, Wu D, Cheon BH, Kim HM, Bouffard J, Yoon JY. N-Heterocyclic Carbene Boranes as Reactive Oxygen Species-Responsive Materials: Application to the Two-Photon Imaging of Hypochlorous Acid in Living Cells and Tissues. *Angew Chem Int Ed* 2018;57:1567-71.
- [29] Pak YL, Park SJ, Song G, Yim Y, Kang H, Kim HM, Bouffard J, Yoon J. Endoplasmic Reticulum-Targeted Ratiometric N-Heterocyclic Carbene Borane Probe for Two-Photon Microscopic Imaging of Hypochlorous Acid. *Anal Chem* 2018;90:12937-43.

- [30] Kenmoku S, Urano Y, Kojima H, Nagano T. Development of a Highly Specific Rhodamine-Based Fluorescence Probe for Hypochlorous Acid and Its Application to Real-Time Imaging of Phagocytosis. *J Am Chem Soc* 2007;129:7313-8.
- [31] Hwang SM, Yun D, Lee H, Kim M, Lim M.H, Kim K.T, Kim C. Relay detection of Zn^{2+} and S^{2-} by a quinoline-based fluorescent chemosensor in aqueous media and zebrafish. *Dyes Pigments* 2019;165:264-72.
- [32] Wang Z, Zhang Y, Song J, Li M, Yang Y, Xu X, Xu H, Wang S. Three novel camphor-based fluorescence probes for ratiometric detection of hypochlorite and bio-imaging in living cells. *Sens Actuators B* 2019;284:148-58.
- [33] Yuan L, Wang L, Agrawalla BK, Park SJ, Zhu H, Sivaraman B, Peng J, Xu QH, Chang YT. Development of Targetable Two-Photon Fluorescent Probes to Image Hypochlorous Acid in Mitochondria and Lysosome in Live Cell and Inflamed Mouse Model. *J Am Chem Soc* 2015;137: 5930-8.”
- [34] Huang Y, Zhang P, Gao M, Zeng F, Qin A, Wu S, Tang BZ. Ratiometric detection and imaging of endogenous hypochlorite in live cells and in vivo achieved by using an aggregation induced emission (AIE)-based nanoprobe. *Chem Commun* 2016;52:7288-91.
- [35] Cimmino A, Evidente A, Mathieu V, Andolfi A, Lefranc F, Kornienko A, Kiss R. Phenazines and cancer. *R Nat Prod Res* 2012;29:487-501.

- [36] Guttenberger N, Blankenfeldt W, Breinbauer R. Recent developments in the isolation, biological function, biosynthesis, and synthesis of phenazine natural products. *Bioorgan Med Chem* 2017;25:6149-66.
- [37] Oni FE, Olorunleke OF, Höfte M. Phenazines and cyclic lipopeptides produced by *Pseudomonas* sp. CMR_{12a} are involved in the biological control of *Pythium myriotylum* on cocoyam (*Xanthosoma sagittifolium*). *Biol Control* 2019;129:109-14.
- [38] Lin ZQ, Xie J, Zhang BW, Li JW, Weng J, Song RB, Huang X, Zhang H, Li H, Liu Y, Xu ZJ, Huang W, Zhang Q. Solution-processed nitrogen-rich graphene-like holey conjugated polymer for efficient lithium ion storage. *Nano Energy* 2017;41:117-27.
- [39] Li G, Gao J, Hu F, Zhang Q. Synthesis, characterization, and physical properties of two novel nonaheteroacene derivatives. *Tetrahedron Lett* 2014;55:282-5.
- [40] Li Y, Wang Z, Zhang C, Gu P, Chen W, Li H, Lu J, Zhang Q. Thiadizoloquinoxaline-Based N-Heteroacenes as Active Elements for High-Density Data-Storage Device. *ACS Appl Mater Interfaces* 2018;10:15971-9.
- [41] Jang K, Brownell LV, Forster PM, Lee DC. Self-Assembly of Pyrazine-Containing Tetrachloroacenes. *Langmuir* 2011;27:14615-20.
- [42] Feng XJ, Tian PZ, Xu Z, Chen SF, Wong MS. Fluorescence-Enhanced Chemosensor for Metal Cation Detection Based on Pyridine and Carbazole. *J Org Chem* 2013;78:11318-25.

- [43] Song X, Zhao J, Zhang W, Chen L. Novel n-channel organic semiconductor based on pyrene-phenazine fused monoimide and bisimides. *Chin Chem Lett* 2018;29:331-5.
- [44] Su JX, Wang XT, Chang J, Wu GY, Wang HM, Yao H, Lin Q, Zhang YM, Wei TB. Colorimetric and fluorescent chemosensor for highly selective and sensitive relay detection of Cu^{2+} and H_2PO_4^- in aqueous media. *Spectrochim. Acta* 2017;182:67-72.
- [45] Wang H, Lu Y. Morphological control of self-assembly polyaniline micro/nano-structures using dichloroacetic acid *Synthetic Metals* 2012;162:1369-74.
- [46] Gowda A, Jacob L, Singh DP, Douali R, Kumar S. Charge Transport in Novel Phenazine Fused Triphenylene Supramolecular Systems. *Chemistry Select* 2018;3:6551-60.
- [47] Zhang HL, Wei TB, Li WT, Qu WJ, Leng YL, Zhang JH, Lin Q, Zhang YM, Yao H. Phenazine-based colorimetric and fluorescent sensor for the selective detection of cyanides based on supramolecular self-assembly in aqueous solution. *Spectrochim Acta* 2017;175:117-24.
- [48] Zhang HL, Li WT, Qu WJ, Wei TB, Lin Q, Zhang YM, Yao H. Mercaptooxazole-phenazine based blue fluorescent sensor for the ultra-sensitive detection of mercury(II) ions in aqueous solution. *RSC Adv* 2017;7:47547-51.

- [49] Zhuang WR, Wang Y, Cui PF, Xing L, Lee J, Kim D, Jiang HL, Oh YK. Applications of π - π stacking interactions in the design of drug-delivery systems. *J Control Release* 2019;294:311-26.
- [50] Zhai C, Zhang P, Peng P, Hou B, Li L. Hydrogen bonding and π - π stacking in nicotinamide/H₂O mixtures. *Spectrochim Acta* 2017;184:294-8.
- [51] Shi HX, Li WT, Li Q, Zhang HL, Zhang YM, Wei TB, Lin Q, Yao H. A novel self-assembled supramolecular sensor based on thiophene-functionalized imidazophenazine for dual-channel detection of Ag⁺ in an aqueous solution. *RSC Adv* 2017;7:53439-44.
- [52] Soni D, Gangada S, Duvva N, Roy TK, Nimesh S, Arya G, Giribabu L, Chitta R. Hypochlorite-promoted inhibition of photo-induced electron transfer in phenothiazine-borondipyrromethene donor-acceptor dyad: a cost-effective and metal-free “turn-on” fluorescent chemosensor for hypochlorite. *New J Chem* 2017;41:5322-33.
- [53] Xu Q, Heo CH, Kim G, Lee HW, Kim HM, Yoon J. Development of Imidazoline-2-Thiones Based Two-Photon Fluorescence Probes for Imaging Hypochlorite Generation in a Co-Culture System. *Angew Chem Int Ed* 2015;127:4972-6.

Table of Contents

Scheme 1 Structure and synthesis of the sensor **POC**.

Figure 1 The response fluorescence intensity **POC** (20 μM) with different volumetric fractions of water (Vol%).

Figure 2 The response fluorescence intensity of **POC** (20 μM) were present and absent ClO^- in DMSO/ H_2O (3:7, v/v) solution. Inset: photograph showing the change in fluorescence color of **POC** after addition of ClO^- (50 equiv.) in DMSO/ H_2O (3:7, v/v) solution.

Figure 3 The response fluorescence intensity of **POC** (20 μM) were present different concentration ClO^- in DMSO/ H_2O (3:7, v/v) solution. Inset: The ratios of emission intensities at 489 and 550 nm (F_{489}/F_{550}) depending on the concentration of ClO^- .

Figure 4 Fluorescent spectra of target compound **POC** (2.0×10^{-5} M) in DMSO/ H_2O (3:7, v/v, 20 μM) solution in the presence of hypochlorite and other analytical substrate (50 equiv.). Inset: photograph showing the change in color of the solution of **POC** in DMSO/ H_2O (3:7, v/v, 20 μM) solution after addition of hypochlorite and other analytical substrate using UV-lamp at room temperature.

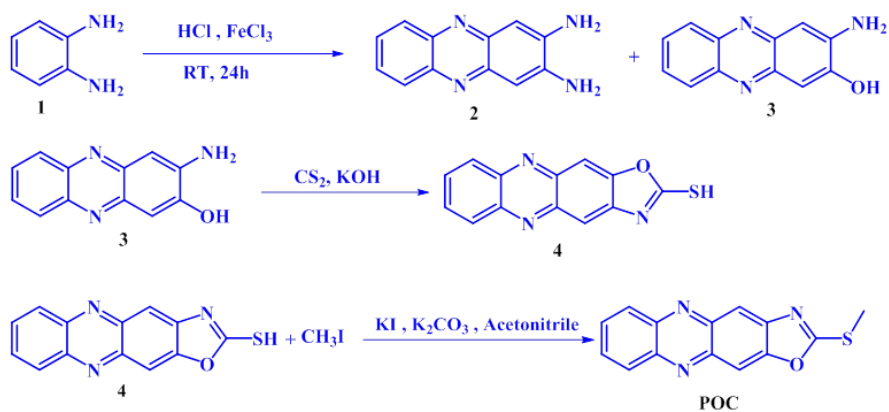
Figure 5 The intensity ratio (F_{489}/F_{550}) for a 1:50 mixture of **POC** (20 μM) and different analytical substrates, in DMSO/ H_2O (3:7, v/v) solution at room temperature. The order of the analytical substrate is: 1 **POC**, 2 ClO^- , 3 F^- , 4 Cl^- , 5 Br^- , 6 I^- , 7 ClO_3^- , 8 BrO_3^- , 9 IO_3^- , 10 HPO_4^{2-} , 11 H_2PO_4^- , 12 PO_4^{3-} ,

13 $\text{P}_2\text{O}_7^{4-}$, 14 $\text{P}_3\text{O}_{10}^{5-}$, 15 HSO_4^- , 16 SO_3^{2-} , 17 SO_4^{2-} , 18 $\text{S}_2\text{O}_3^{2-}$, 19 S^{2-} , 20 SCN^- , 21 N_3^- , 22 NO_3^- , 23 NO_2^- , 24 $\text{C}_2\text{O}_4^{2-}$, 25 CO_3^{2-} , 26 AcO^- , 27 $\text{B}_4\text{O}_7^{2-}$ and 28 H_2O_2 .

Figure 6 Job's plot examined between **POC** and ClO^- , indicating the 2:1 stoichiometry.

Scheme 2 Chemical structures and cartoon representations of **POC** and ClO^- and the reaction mechanism in this system.

Figure 7 Partial ^1H NMR spectra of **POC** ($\text{DMSO-}d_6$) and in the presence of varying amounts of hypochlorite.



Scheme 1 Structure and synthesis of the sensor **POC**.

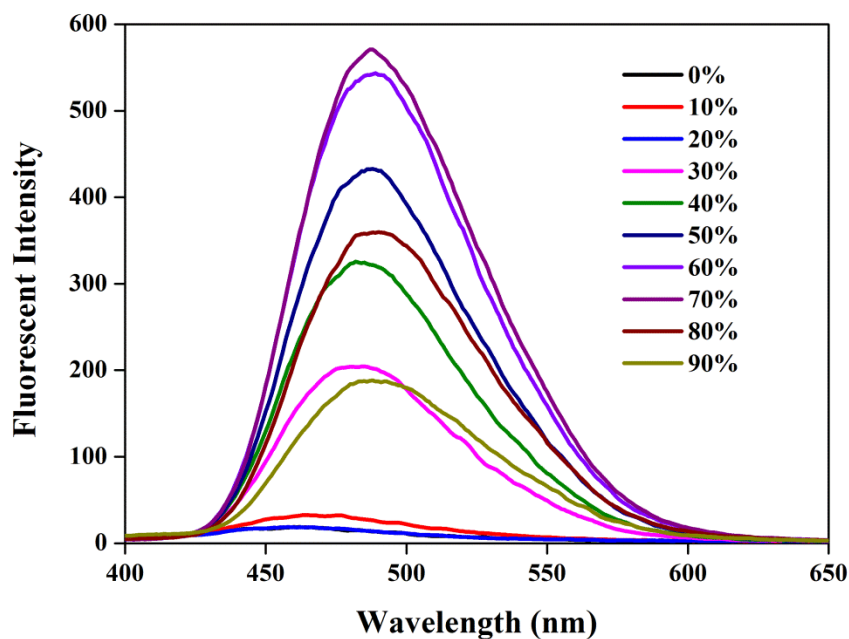


Figure 1 The response fluorescence intensity **POC** (20 μM) with different volumetric fractions of water (Vol%).

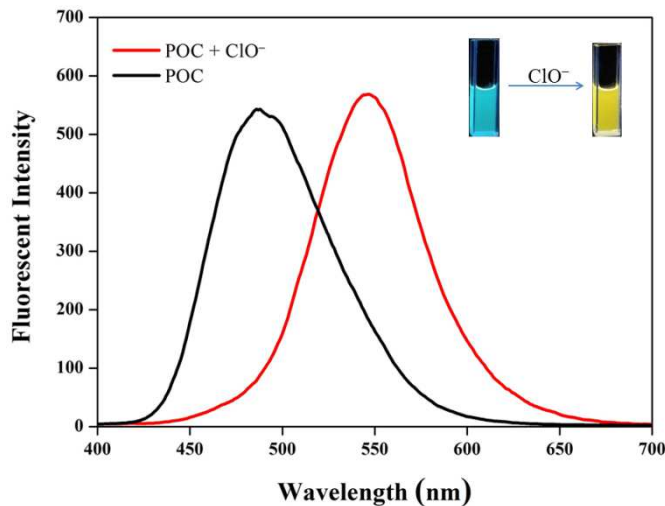


Figure 2 The response fluorescence intensity of **POC** (20 μM) were present and absent ClO^- in DMSO/ H_2O (3:7, v/v) solution. Inset: photograph showing the change in fluorescence color of POC after addition of ClO^- (50 equiv.) in DMSO/ H_2O (3:7, v/v) solution.

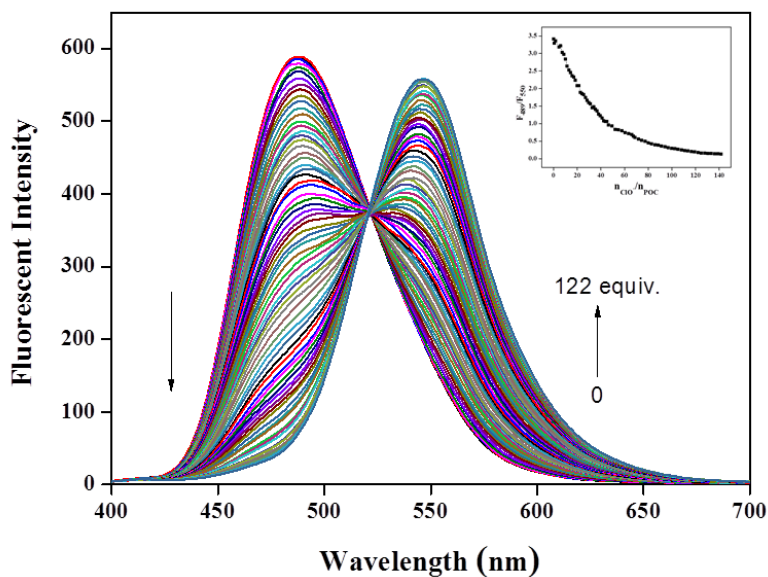


Figure 3 The response fluorescence intensity of **POC** (20 μM) were present different concentration ClO^- in DMSO/ H_2O (3:7, v/v) solution. Inset: The ratios of emission intensities at 489 and 550 nm (F_{489}/F_{550}) depending on the concentration of ClO^- .

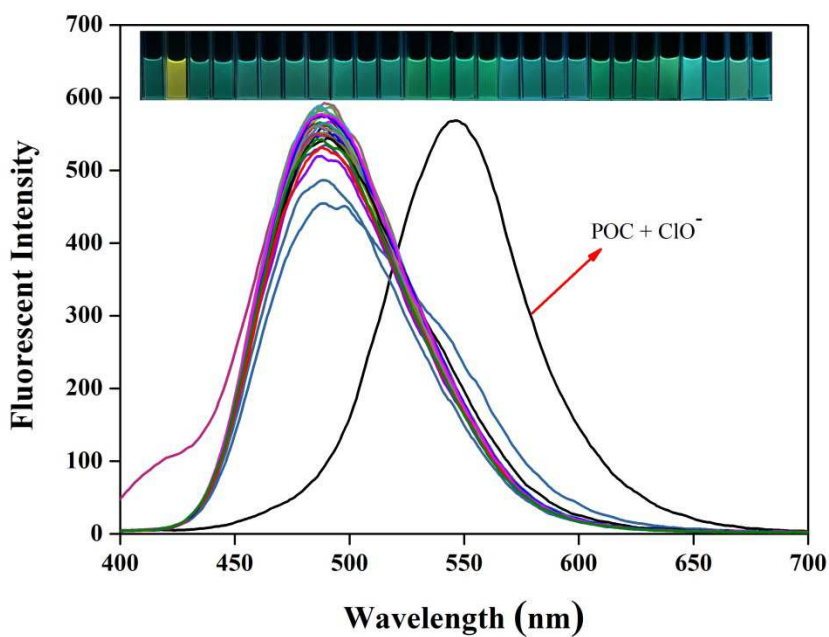


Figure 4 Fluorescent spectra of target compound **POC** (2.0×10^{-5} M) in DMSO/ H_2O (3:7, v/v, 20 μM) solution in the presence of hypochlorite and other analytical substrate (50 equiv.). Inset: photograph showing the change in color of the solution of **POC** in DMSO/ H_2O (3:7, v/v, 20 μM) solution after addition of hypochlorite and other analytical substrate using UV-lamp (365 nm) at room temperature.

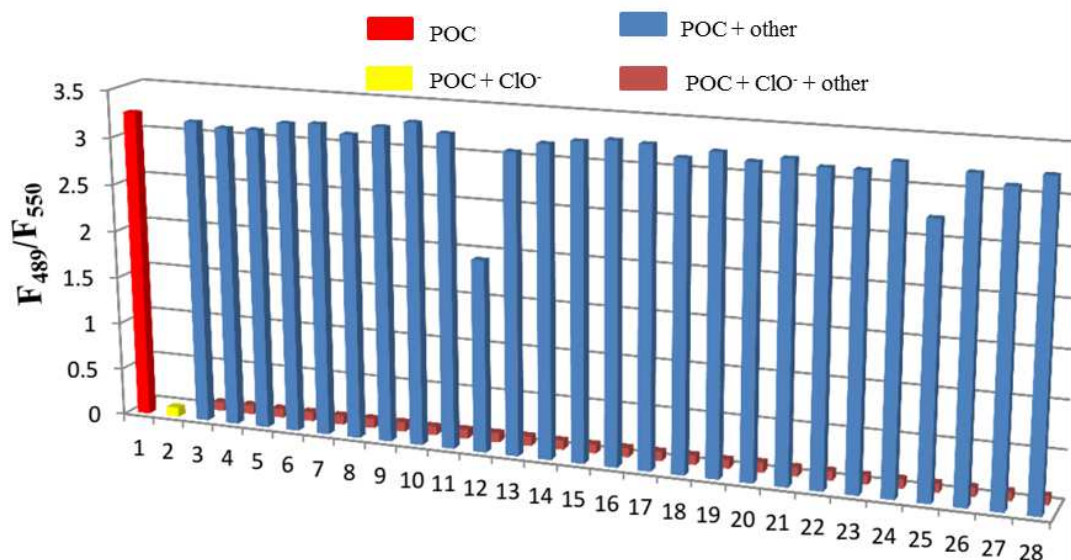


Figure 5 The intensity ratio (F_{489}/F_{550}) for a 1:50 mixture of **POC** (20 μM) and different analytical substrates in DMSO/ H_2O (3:7, v/v) solution at room temperature. The order of the analytical substrate is: 1 POC, 2 ClO^- , 3 F^- , 4 Cl^- , 5 Br^- , 6 I^- , 7 ClO_3^- , 8 BrO_3^- , 9 IO_3^- , 10 HPO_4^{2-} , 11 H_2PO_4^- , 12 PO_4^{3-} , 13 $\text{P}_2\text{O}_7^{4-}$, 14 $\text{P}_3\text{O}_{10}^{5-}$, 15 HSO_4^- , 16 SO_3^{2-} , 17 SO_4^{2-} , 18 $\text{S}_2\text{O}_3^{2-}$, 19 S^{2-} , 20 SCN^- , 21 N_3^- , 22 NO_3^- , 23 NO_2^- , 24 $\text{C}_2\text{O}_4^{2-}$, 25 CO_3^{2-} , 26 AcO^- , 27 $\text{B}_4\text{O}_7^{2-}$ and 28 H_2O_2 .

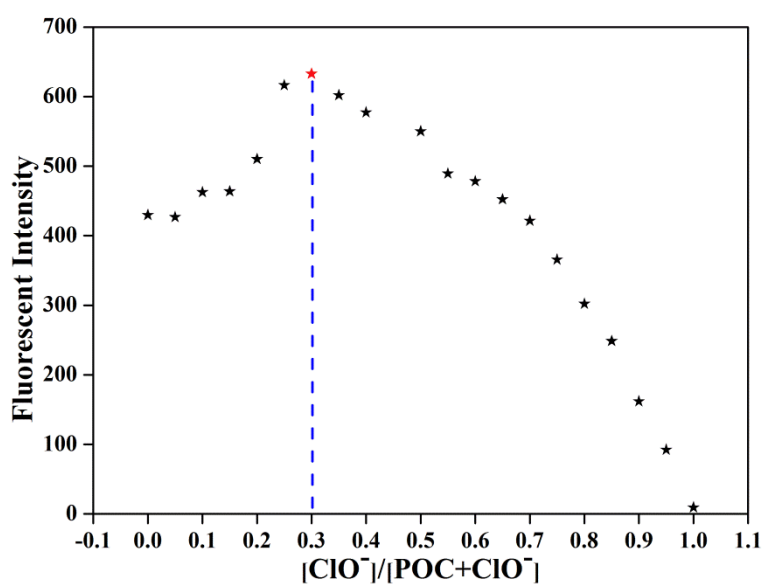
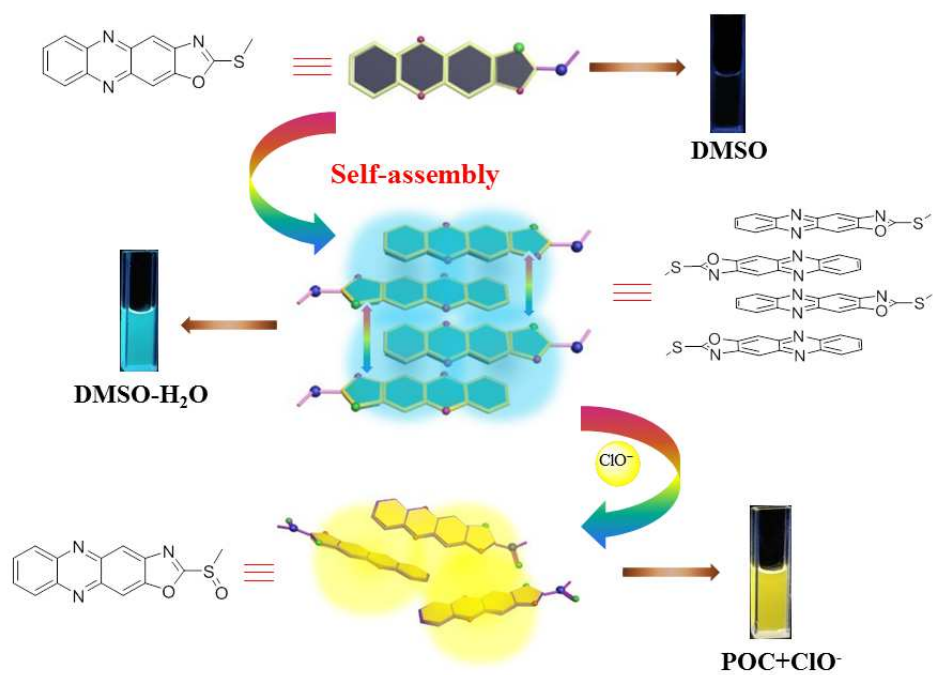


Figure 6 Job's plot examined between **POC** and ClO^- , indicating the 2:1 stoichiometry.



Scheme 2 Chemical structures and cartoon representations of **POC** and ClO^- and the reaction mechanism in this system.

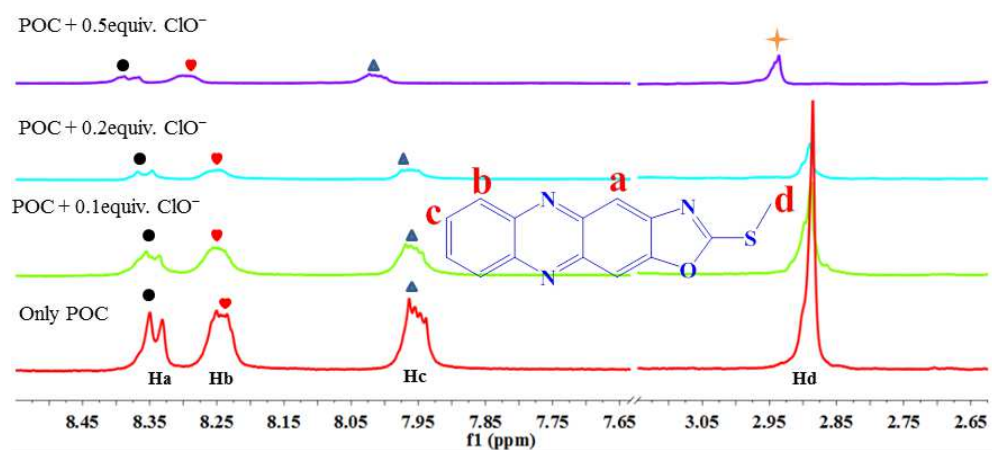


Figure 7 Partial ^1H NMR spectra of **POC** ($\text{DMSO-}d_6$) and in the presence of varying amounts of hypochlorite.

Highlights

1. A novel fluorescent sensor for highly selective and sensitive detection of hypochlorite.
2. Taking advantage of a simple mechanism of oxidation reaction.
3. The test strips could conveniently and rapidly detect hypochlorite solutions.
4. POC could serve as a fluorescent sensor material for detecting the active ingredient in 84 disinfectant.